International Journal of Transportation Science and Technology xxx (xxxx) xxx

Contents lists available at ScienceDirect

International Journal of Transportation Science and Technology

journal homepage: www.elsevier.com/locate/ijtst

Comparing the vibrational behaviour of e-kick scooters and e-bikes: Evidence from Italy

Roberto Ventura [a], Andrea Ghirardi [a], David Vetturi [b], Giulio Maternini [a], Benedetto Barabino [a,*]

[a] Department of Civil, Environment, Land and Architecture Engineering and Mathematics (DICATAM), University of Brescia, Brescia 25123, Italy
[b] Department of Mechanical and Industrial Engineering (DIMI), University of Brescia, Brescia 25123, Italy

ARTICLE INFO

Article history:
Received 23 December 2022
Received in revised form 25 July 2023
Accepted 28 October 2023
Available online xxxx

Keywords:
E-kick scooters vibrational behaviour
E-bike vibrational behaviour
Artificial Neural Network
Monte Carlo simulation
Soft mobility

ABSTRACT

E-kick scooters are currently among the most popular emerging electric-powered Personal micro–Mobility Vehicles (e-PMVs) and have recently been equated to e-bikes. However, even if the dynamic behaviour of e-bikes is well studied, much less has been done to understand the behaviour of e-kick scooters. Furthermore, comparisons between the two vehicles have rarely been investigated and only based on mechanical models.

This study covers this gap by proposing a novel framework that evaluates the vibrational behaviours of both vehicles when driven by different users and exposed to the pavement irregularities, using both real and simulated data. The experimental data are collected equipping an e-kick scooter and an e-bike with Inertial Measurement Units, and then processed by ISO 2631–1 method to obtain an objective evaluation of the comfort. Next, the experimental data are expanded to include uncertainty applying a Monte Carlo Simulation based on a two-layer feed-forward Artificial Neural Network. Afterwards, several statistical analyses are performed to understand the key factors affecting the vibrational magnitude (and their extent) for each vehicle. This framework was tested in an Italian city (Brescia) along urban paths with five different pavement surfaces.

The results showed that the e-kick scooter appears to be globally more solicited than the e-bike in terms of vibrational magnitude. Moreover, pavement surface, sensor position, user gender, user height, and travel speed are identified as crucial factors explaining the vibrational magnitude for both vehicles.

The overall findings challenge the recent European regulations that equated e-kick scooters with bikes. These findings may help public administrations in planning the circulation of e-bikes and e-kick scooters in cities and recommend that manufacturers improve the e-kick scooter design by including shock absorbers to increase comfort.

1. Introduction

Nowadays, electric-powered Personal Mobility Vehicles (e-PMVs) are an emerging technology for which a growing interest is observed. These are soft mobility vehicles that generally include e-bikes, e-kick scooters, and self-balancing devices, *i.e.*, all vehicles characterized by small size and compactness (Carrara et al., 2021). They are usually equipped with electric motors powered by a rechargeable battery and are cost-effective if used for covering short distances within a city

* Corresponding author.
E-mail address: benedetto.barabino@unibs.it (B. Barabino).

https://doi.org/10.1016/j.ijtst.2023.10.010
2046-0430/

Please cite this article as: R. Ventura, A. Ghirardi, D. Vetturi et al., Comparing the vibrational behaviour of e-kick scooters and e-bikes: Evidence from Italy, International Journal of Transportation Science and Technology, https://doi.org/10.1016/j.ijtst.2023.10.010

(Boglietti et al., 2021). The diffusion of e-PMVs can be traced back to 2017 in the USA, and a few years later in many of Europe's largest cities (e.g., Barcelona, Milan, and Paris), where e-scooter sharing services have grown exponentially, mainly with the goal to serve as first/last mile connections to transit services (Tzouras et al., 2022; Azimi et al., 2021). Afterwards, the extensive measures taken by many developed nations for the promotion of cycling, e-scootering, and walking in response to the COVID-19 pandemic crisis further propelled the popularity of e-PMVs (Abdullah et al., 2022; Wang et al., 2021). However, this diffusion has led to relevant issues. At the metropolitan scale, issues concern the impact of these devices on the environment and public transport management. At the city level, related issues regard the impact of e-PMVs on mobility, urban planning, and road safety (Boglietti et al., 2021).

Specifically, in cities where e-PMVs are most used, there is a growing number of crashes involving these vehicles, raising several concerns about the lack of specific regulations (Bloom et al., 2020). Therefore, several corrective actions have been taken in some European countries, issuing regulations for allowing the circulation of e-PMVs (e.g., Danish: Executive order n.40 of 14 January 2019; French: Decree n. 2019–1082 of 23 October 2019, German: Regulation n.21 of 14 June 2019; Italian: Decree 30 December 2019, n.162). Some of them, including the Italian Decree, equated e-kick scooters with e-bikes and introduced specific indications regarding their circulation in urban areas both on cycling paths and traditional roads. Specifically, in Italy, until 2019, the Traffic Code did not explicitly regulate the circulation of e-kick scooters (Repubblica Italiana, 2015). Consequently, such vehicles could not run on public roads but exclusively in private areas (Maternini, 2020). At the end of 2019, Italian Law No. 162/2019 regulated the circulation of e-kick scooters for the first time, equating those with an electric motor not exceeding 0.50 kW with bicycles (Repubblica Italiana, 2019). Subsequently, other pieces of legislation followed (Repubblica Italiana, 2021; Repubblica Italiana, 2022). Nowadays, according to current Italian legislation, riding e-kick scooters is allowed only for users who are at least 14 years old: 1) On urban roads characterised by a speed limit of 50 km/h, only if bikes are allowed, and with a maximum speed of 20 km/h; 2) On rural roads, only if there is a bike lane, and exclusively on the latter; 3) Within pedestrian areas with a maximum speed of 6 km/h.[1]

However, all these regulations were suddenly introduced owing to the uncontrolled invasion of e-kick scooters, without mature studies to support them. Moreover, e-kick scooters and bikes (or e-bikes) differ with respect to the trip patterns and from a technical viewpoint.

As for trip patterns, studies showed that the average travel speed of e-kick scooters is lower than that of e-bikes (i.e., $7 \div 10$ km/h *vs* $10 \div 12$ km/h); moreover, e-kick scooters are typically used to travel shorter distances than e-bikes (i.e., $0.5 \div 5$ km *vs* $0.5 \div 15$ km) (Almannaa et al., 2021; Zagorskas and Burinskienė, 2020).

As for the design features, e-bikes have large wheels and tyres, which could generate a stabilising gyroscopic effect and dissipate the shocks induced by the surface irregularities. Contrarywise, e-kick scooters are generally equipped with small diameter wheels, which may not be able to induce significant stabilising and dissipative effects. Other differences concern the subsistence of divergent vehicle-rider system schemes, with the different position of the mass centre during the ride: higher in e-kick scooters than in e-bikes. All these factors could easily lead to different behaviours to be investigated, depending on the physical characteristics of the urban environment and the road surface.

The behaviour of bikes and motorbikes is a well-known research topic on vehicle dynamics (e.g., Sharp, 1971; Cossalter et al., 2006; Meijaard et al., 2007; Chen et al., 2009). For instance, the relationship between pavement quality and perceived comfort, through the assessment of vibrational behaviour, is a well-studied topic, usually in relation to the vehicle speed (e.g., Feizi et al., 2020; Gao et al., 2018).

Conversely, much less evidence is reported for e-kick scooters' dynamics. Only a handful of studies explored the influence of e-kick scooters' vibrations on human health and comfort (Cano-Moreno et al., 2019; Cano-Moreno et al., 2021), the risk factors affecting safety while riding (Lee et al., 2021), the dynamics of e-kick scooters and users during a ride (Vetturi et al., 2023; Garman et al., 2020) and the longitudinal, lateral, and vertical motion of a benchmark e-kick scooter (García-Vallejo et al., 2020).

Nevertheless, according to the retrieved literature, no experimental prior attempt has been made to investigate the relationship between pavement and user characteristics and vibrational behaviour of e-kick scooters and e-bikes by a comparative study. This study covers the former gap. Specifically, this study builds on Boglietti et al. (2022) by proposing a novel framework to compare the vibrational behaviour of these vehicles. This comparison is aimed at performing an objective evaluation of the user comfort while riding, by ISO 2631–1 evaluation method. This framework integrates Artificial Neural Network (ANN), Monte Carlo Simulation (MCS) and Multiple Linear Regression (MLR) models together. First, the magnitude of the vibrational behaviour is analysed through experimental accelerometric data. Next, unlike Boglietti et al. (2022), the proposed framework enables extending a sample of experimental data by applying MCS technique for accounting the statistical uncertainty. MCS technique is applied on a two-layer feed-forward ANN previously trained on the data acquired during the experimental trials. The use of an ANN tool responds to the need for fitting a computational model with a high predictive performance to be exploited for the generation of new simulated data. Finally, simulated data are analysed using MLR models to understand which factors affect this vibrational magnitude (and their extent) for each vehicle.

This framework is tested in the city of Brescia (Italy) and considered 168 experimental and 10′000 simulated trials, on several rides of e-kick scooters and e-bikes along urban paths characterised by different pavement surfaces.

[1] At the time this article was revised (July 2023), the Italian government was passing a new measure (not yet officially published) that would require mandatory license plates, the use of helmets and insurance, and a ban on parking on sidewalks starting January 1, 2024.

This study aims to contribute to both theory and practice.

From a theoretical viewpoint, although the proposed framework integrates widely known analysis tools, it covers a research area that has remained unaddressed, so far, advancing the knowledge related to the dynamic vibrational behaviour of e-kick scooters and e-bikes according to a comparative analysis. Thus, an explicit indication of key determinants affecting the vibrational magnitude acting on e-kick scooters and e-bikes is provided. Since the vibrational response of a vehicle is strictly related to the comfortability perceived by drivers and to their safety, this knowledge is fundamental to understanding, *e.g.*: 1) the different behaviour adopted by several user categories when choosing the first/last mile transport mode (e.g., Azimi et al., 2021); 2) The different crash risk observed for several user categories when driving e-PMVs on different surfaces (e.g., Tian et al., 2022; Stigson et al., 2021).

On the practical perspective, recognising different vibrational behaviours (if any) may challenge recent European regulations that equated e-kick scooters with e-bikes and provide useful information for planning. For instance, some paths designed according to e-bikes' technical characteristics could be revised to improve the safety and the comfortability of the users, if intended for e-kick scooters. In addition, different dynamic behaviours can suggest some technical improvements to the design of vehicles in terms of e.g., shock absorbers.

The remainder of this paper is as follows. Section 2 reviews key literature about vibration behaviour of e-bikes and e-kick scooters. Section 3 illustrates the overall framework for the comparison of vibration behaviour of both vehicles. Section 4 reports the experiments and findings of this framework on a real case study and provides some recommendations. Finally, Section 5 provides conclusions and future perspectives.

2. Literature review

The dynamic behaviour of two-wheeled vehicles is a well-known research topic. In most cases, the aim is to evaluate comfort and safety through the response of the vehicle to the roughness of the road surface, usually assessed by a measurement of the vibrations absorbed by the vehicle or user (Bíl et al., 2015; Chou et al., 2015; Gao et al., 2018; Feizi et al., 2020). On the one hand, the most studied two-wheeled vehicles were motorcycles, for which the relationship among vehicles' design characteristics, surface type, and riding performance is currently well known. For instance, past research showed that vibrational behaviour mainly depends on suspension and tyre characteristics (Frendo et al., 2002; Cossalter et al., 2006), motor power supply (Mulla et al., 2019), usage, unevenness of the road surface and the riding speed (Chen et al., 2009). On other hand, the dynamic behaviour of e-bikes and e-kick scooters is much less studied. To trace a complete background of it, studies have been summarised in Table 1, which is commented in what follows for the main points.

First, analytical research includes studies in which the outcomes derive purely through mechanical modelling and often the model itself is the output of the research. Conversely, empirical research covers studies where the outcomes derive from the processing of collected experimental data.

Second, in analytical studies each datum is simulated through the proposed mechanical model; experimental data are eventually collected only to validate the model. By contrast, in empirical studies inertial Measurement Unit (IMU) sensors were used to collect real acceleration data from on-site riding tests, usually combining Global Positioning System (GPS) to tracking path, and tachometer Revolutions Per Minute (RPM) sensors, to record the riding speed.

Third, different analysis tools were used. In analytical studies, motion analysis tools are used for the construction of the mathematical model. In empirical studies, statistical tools were used for the understanding of the relationships between the collected data and the related factors to discover the effects on safety and comfort. Because the proposed article starts from empirical data, the analysis tools used in analytical studies will not be reported in depth. Specifically, as for empirical studies, some processed vibrational acceleration data according to norms ISO 2631–1 and ISO 2631–5 to evaluate riding comfort (e.g., Gao et al., 2018; Gao et al., 2019). ISO 2631–1 provided a general method to evaluate human exposure to whole-body vibration. ISO 2631–5 proposed an additional method for the evaluation of the effect on health of vibration containing multiple shocks, such as lumped obstacles like potholes, steps, and other significant irregularities in the road surface. When ISO 2631 was not followed, a new evaluation index for comfort is proposed processing acceleration data through customised mathematical procedures (Chou et al., 2015). In some cases, the acceleration data were processed through statistical techniques (e.g., linear regression and ANOVA analysis) and returned the effect between the acceleration and several predictors (Gao et al., 2019). In some cases, the analyses were supported using z-test or t-test to show if the average values of two populations (e.g., e-kick scooters and bikes braking distances, or experienced and inexperienced users) are significantly different (e.g., Feizi et al., 2020; Vetturi et al., 2023). Conversely, none of the previous studies had adopted the ANN tool for modelling the dynamic behaviour of e-bikes and e-kick scooters, although it could be efficiently exploited to fit a computational model with a high predictive performance. Nevertheless, the ANN is a well-known computational model extensively applied in transportation engineering. For instance, it has been successfully exploited for determining engine performance and emission (Tuan Hoang et al., 2021); predicting road traffic accident severity (Shaik et al., 2021); optimising transportation infrastructure maintenance processes (Gharehbaghi, 2016); modelling the traffic flow at a road intersection (Olayode et al., 2021); detecting road pavement defects (Yang et al., 2021). Similarly, there is no evidence on the use of MCS technique to extend the experimental data adopted for the analysis of e-kick scooter and e-bike dynamic behaviour, though there are several applications of the MCS technique in transportation engineering, such as for the optimisation of traffic light cycles (Jiang et al.,

Table 1
E-kick scooter and bike studies related to comfort and safety.

Authors (Year)	Location	Vehicle	Approach	Data sources	Analysis Tools	Relevant Insights/outcomes
Vetturi et al., 2023	Brescia, Italy	e-kick scooter; e-bike	Empirical	Cameras	Kinematic analysis, descriptive statistics, and multiple regression	Comparing the kinematic performance of micro-mobility vehicles during braking
Boglietti et al., 2022	Brescia, Italy	e-kick scooter; e-bike	Empirical	IMU	ISO 2631 methods	Comparing the vibrational behaviour of the two vehicles consideration different users and road surfaces.
Asperti et al., 2021	Milan, Italy	e-kick scooter	Analytical	Test bench (only for model validation)	Single contact point model (for road) and lumped parameter model (for e-scooter)	Planar model for the simulation of the vertical dynamics of an e-scooter, validated for obstacles with experimental data
Cano-Moreno et al., 2021	Madrid, Spain	e-kick scooter	Analytical	Simulated data	Multiple regression	Evaluation of vibration impact on health
Lee et al., 2021	South Korea	e-kick scooter	Empirical	Direct survey	Cluster analysis	Danger level values (also related to surface type) and frequency values
Feizi et al., 2020	Kalamazoo, Michigan, USA	Bike	Empirical	IMU, RPM, GPS, LASER, cameras, and survey	Fault tree analysis, z-test	Assessment method of relationship between skill level and riding performance
García-Vallejo et al., 2020	Spain	e-kick scooter	Analytical	Design parameters of an e-scooter	Multibody dynamic simulation	E-scooter benchmark, compared with a bike benchmark taken from literature.
Garman et al., 2020	Phoenix, Arizona, USA	e-kick scooter	Empirical	IMU, RPM, GPS, and cameras	Descriptive statistics	Maximum values of manoeuvrability and braking distance on different surfaces
Cano-Moreno et al., 2019	Madrid, Spain	e-kick scooter	Analytical	n.a.	Multibody dynamic simulation	Assessment method of vibration impact on health and two models with different vehicle rigidity
Gao et al., 2019	Xi'an, China	Bike	Empirical	IMU, GPS and road surfaces scanning	ISO 2631 methods and linear regression	Correlation between cycling comfort and road surface roughness
Gao et al., 2018	Xi'an, China	Bike	Empirical	IMU, GPS and direct survey	ISO 2631 methods	Comfort evaluation combining vibration measurement and users' perceptions.
Bíl et al., 2015	Olomouc, Czech Republic	Bike	Empirical	IMU and GPS	Comfort synthetic index and linear regression	Dynamic Comfort Index and comfort map of an historical centre
Chou et al., 2015	Taiwan	Bike	Analytical and empirical	IMU, GPS and Inertial profiler	Multibody dynamic simulation and descriptive statistics	Measuring riding smoothness on different surfaces from real or simulated data

2020), for the analysis of the road (Wach, 2014) and air traffic accidents (Stroeve et al., 2009), for traffic speed forecasting (Jeon and Hong, 2016) and for the simulation of traffic loading on bridges (Enright and O'Brien, 2013).

Finally, relevant insights and/or outcomes were considered. These may be both practical results, mainly concerning vehicle comfort, safety, and riding smoothness. Specifically, as for bikes, several studies showed that vibrations increase at increasing speed (e.g., Bíl et al., 2015; Gao et al., 2018). In addition, the macrostructure and properties of the road surface are crucial for vibrations on bikes (Chou et al., 2015). Particularly, uneven old stone pavements and damaged roads are the most uncomfortable surfaces (Bíl et al., 2015). Much less can be said for e-kick scooters' dynamics. For instance, assessing the influence of e-kick scooters' vibrations on human health, pavement type and speed has been identified as the main variables affecting the vibration level, like for bikes (Cano-Moreno et al., 2019; Cano-Moreno et al., 2021). Furthermore, others investigated the dynamics behaviour of e-kick scooters against an e-bike, although only at analytical level (García-Vallejo et al., 2020). The results showed that, unlike the e-bike, the e-kick scooter was unstable at any speed, hence, it could never be ridden without the use of hands. Moreover, someone developed a method to help define suspension geometries and insulation layers between the frame and the rider to enhance the riding comfort level, but it has not yet been applied (Asperti et al., 2021). Only Boglietti et al. (2022) compared the vibrational response (which can affect users' comfort and safety during a ride) of e-kick scooters and e-bikes at the pavement irregularities, using a small sample of real data. Preliminary results showed that e-kick scooters are globally less comfortable than the e-bikes. Lastly, empirical studies are still occasional and mainly focused on manoeuvrability, braking distance, and riding environment hazard levels (Garman et al., 2020; Yang et al., 2021; Vetturi et al., 2023).

Undoubtedly, all these studies have contributed to the analysis of vibrational behaviour on separate vehicles and provided valuable results. However, some gaps persist. First, no empirical study has been made to compare the dynamic behaviour of e-bikes and e-kick scooters in terms of vibrational acceleration, or rather in terms of comfort. Although Boglietti et al. (2022) provided a first attempt for this evaluation, they adopted only a limited sample of real data without a data expansion to account for statistical uncertainty. Moreover, they did not investigate the effect that user characteristics (i.e., gender, age, height, and mass) could have on vibrational magnitude. Second, there is no research that compares e-kick scooters and e-bikes to identify the key factors that may affect the magnitude of vibrations.

This paper aims to cover the former gaps applying the MCS and the ANN to extend the experimental data adopted for the analysis of e-kick scooter and e-bike vibrational behaviour. In addition, MLR will show the effect of significant variables on the vibrational behaviour.

3. Framework

The framework for the comparison of the e-kick scooter and e-bike vibrational behaviour is synthetised in the flowchart shown in Fig. 1, that adopts the symbols provided by the American National Standards Institute (ANSI). The procedure is summarised in several steps, which are individuated with a dashed line and are described and formulated in what follows.

STEP 1: Raw data acquisition from experimental trials

According to STEP 1, the framework starts with the acquisition of experimental raw data related to the accelerations acting on the e-kick scooter and e-bike during several trials, by Inertial Measurement Units (IMUs) sensors. More precisely, let:

- I be the set of experimental trials and $i \in I$ be the generic trial.
- J be the set of Cartesian axes (x, y, z) and $j \in J$ be the generic axis.
- M be the set of trial explanatory variable indices and $m \in M$ the generic index.
- e_m be the m^{th} explanatory variable and e_{im} be the value of the m^{th} explanatory variable observed in trial $i \in I$.
- $\overline{\overline{E}}_{obs} = \left[e_{i1}, e_{i2} \cdots, e_{im} \cdots, e_{i|M|}\right] \in R^{|I|,|M|} \quad (\forall i \in I; \forall m \in M)$ be the matrix of the explanatory variable's values $e_{im} (\forall i \in I; \forall m \in M)$ observed in set I.
- $a_{ij}(t)\left[m/s^2\right]$ be the acceleration acting along the IMU's reference axis $j \in J$ as a function of time t, during trial $i \in I$.
- $f_s[Hz]$ be the IMU's sampling frequency.
- $T_i[s]$ be the time duration of the trial $i \in I$.
- U_i be the set of the time sampling index of the trial $i \in I$ and $u \in U_i$ be the generic time sampling index.
- $t_{iu}[s]$ be the u^{th} sampling time of the trial $i \in I$ $(\forall u \in U_i)$.
- $\overline{\overline{A}}_i = \left[a_{ix}(t_{iu}) a_{iy}(t_{iu}) a_{iz}(t_{iu})\right] \in \mathbb{R}^{|U_i|,3} (\forall u \in U_i)$ be the matrix of the accelerations data measured during the trial $i \in I$.

First, for the characterisation of the vibrational dynamic behaviour, a set of experimental trials (I) should be performed. Kinematic measurements should be carried by IMUs equipped with accelerometers and firmly fixed to the vehicular frames. Research tests should involve users selected to ensure a good variability in terms of age, mass, height, and level of experience with e-kick scooters and e-bikes. They should be asked to ride the two vehicles along different paths, characterised by surfaces with different levels of irregularity. The path length should be representative of typical journeys made by e-kick scooter and e-bike users. The users should be instructed to move along the paths at predetermined speeds to ensure consistency between different trials. The constraint of the predetermined speed could be removed if the vehicles are equipped with GPS sensors to determine the average speed of each trip.

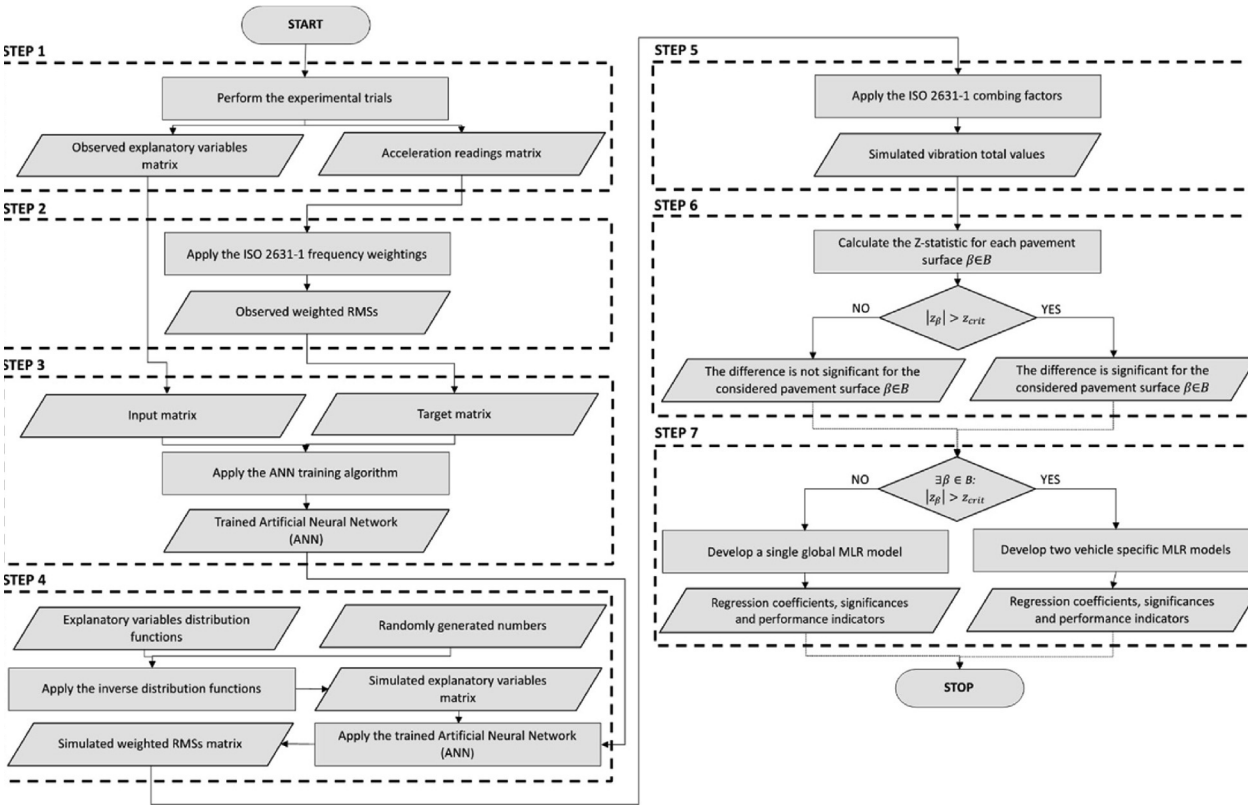

Fig. 1. Flowchart of the proposed evaluation framework.

Second, a set of explanatory variables $e_m(\forall m \in M)$ should be identified for the set of experimental trial I, and the corresponding observed values e_{im} $(\forall i \in I; \forall m \in M)$ should be recorded for each trial $i \in I$. These variables should be selected to ensure a good description of the trial boundary conditions, such as the surface typology, the vehicle typology, the sensor position, the user characteristics (e.g., gender, age, height, mass) and the travel speed. These could be a continuous variable (e.g., user height, user mass, travel speed), a discrete variable (e.g., user age, user gender), or a categorical variable (e.g., surface typology, vehicle typology, sensor position, user gender). Collecting the variable values observed in each test, the matrix of the observed explanatory factors ($\bar{\bar{E}}_{obs}$) can be obtained.

Third, during each trial $i \in I$, acceleration data acting along the three IMUs' reference axis $(a_{ij}(t) \forall j \in J)$ should be recorded as a function of time t. The accelerations are sampled by the sensors with a sampling frequency f_s, then the sampling times t_{iu} can be computed as indicated in Eq. (1). This implies that the data recordings are discrete over time $(a_{ij}(t_{iu}))$.

$$t_{iu} = \frac{u}{f_s}[s] \ \forall i \in I \forall u \in U_i \tag{1}$$

Collecting the acceleration values measured along each axis $j \in J$ and in each sampling time, a matrix of acceleration data $(\bar{\bar{A}}_i)$ can be obtained for each trial $i \in I$.

STEP 2: ISO 2631–1 evaluation method

Next, according to STEP 2, the raw acceleration data acquired in STEP 1 are processed adopting the ISO 2631–1 to evaluate the rider exposure to whole-body vibration when riding the vehicles. This method prescribes frequency weightings for the computation of the weighted Root Mean Square (RMS) acceleration acting along the three IMUs' reference axis. This RMS index makes it possible to estimate, from the vibration magnitude, frequency and direction, the relative effects on comfort of different types of vibration. More formally, let:

- $aw_{ij}(t)\left[m/s^2\right]$ be the weighted acceleration acting along the IMU's reference axis $j \in J$ as a function of time t, for the trial $i \in I$.
- $RMS_{aw_{ij}}\left[m/s^2\right]$ be the weighted RMS associated with acceleration acting along the IMU's reference axis $j \in J$ during the trial $i \in I$.

Table 2
Parameters for the frequency weightings prescribed for the prediction of the effects of vibration on comfort (ISO, 1997).

Weighting	Band limiting		Acceleration-velocity transition			Upward step			
	$f_1[Hz]$	$f_2[Hz]$	$f_3[Hz]$	$f_4[Hz]$	Q_4	$f_5[Hz]$	Q_5	$f_6[Hz]$	Q_6
W_k	0.4	100	12.5	12.5	0.63	2.37	0.91	3.35	0.91
W_d	0.4	100	2.0	2.0	0.63	∞	-	∞	-

- $A_{ij}(f)\ [m/s^2]$ be the acceleration acting along the IMU's reference axis $j \in J$ as a function of the frequency f, for the trial $i \in I$, i.e., the Fourier transform of the signal $a_{ij}(t)$ (frequency domain).
- $f_1, f_2, f_3, f_4, f_5, f_6$ and Q_4, Q_5, Q_6 be the frequencies and resonance quality factors respectively, that are parameters of the transfer function, which determines the overall frequency weighting (see Table 2).
- $H_h(f)$ be the transfer function of the high pass filter.
- $H_l(f)$ be the transfer function of the low pass filter.
- $H_t(f)$ be the transfer function of the acceleration-speed transition filter (proportionality to acceleration at lower frequencies, proportionality to speed at higher frequencies).
- $H_s(f)$ be the transfer function of the upward step filter (proportionality to jerk, i.e., to the third derivative of the position vector with respect to time).
- $H(f)$ be the total transfer function for health and comfort frequency weighting.
- $Aw_{ij}(f)\ [m/s^2]$ be the weighted acceleration along the IMU's reference axis j ($\forall j \in J$) as a function of the frequency f, acting during the trial $i \in I$.
- r be the generic row index of the discrete Fourier transform.
- $\bar{r}_i$ be the number of the non-redundant discrete Fourier transform frequency rows for the trial $i \in I$.
- f_{ir} [Hz] be the frequency associated at the r^{th} row of the discrete Fourier transform for the trial $i \in I$.

Because the way in which vibration affects the comfort is dependent on the vibration frequency content, different frequency weightings are prescribed by the ISO 2631–1 for the different axes of vibration: W_d for x and y axes and W_k for z axis. The weighted RMS associated with acceleration measured along the three IMUs' reference axes during each trial should be computed in time domain as indicated in Eq. (2), where the transition from the integral to the summation is due to the approximation introduced by the sampling discretization.

$$RMS_{aw_{ij}} = \left(\frac{1}{T_i}\cdot\int_0^{T_i} aw_{ij}^2(t)dt\right)^{\frac{1}{2}} \approx \left(\frac{1}{|U_i|}\cdot\sum_{u\in U_i} aw_{ij}^2(t_{iu})\right)^{\frac{1}{2}} [m/s^2]\ \forall i \in I \forall j \in J \tag{2}$$

According to ISO 2631–1, the frequency weightings can be performed in the frequency domain through the implementation of digital filters mathematically expressed by the total transfer function for health and comfort ($H(f)$), defined as follows.

$$H_h(f) = \sqrt{\frac{f^4}{f^4+f_1^4}} \tag{3}$$

$$H_l(f) = \sqrt{\frac{f_2^4}{f^4+f_2^4}} \tag{4}$$

$$H_t(f) = \sqrt{\frac{f^2+f_3^2}{f_3^2}}\cdot\sqrt{\frac{f_4^4 Q_4^2}{f^4Q_4^2+f^2f_4^2\left(1-2Q_4^2\right)+f_4^4Q_4^2}} \tag{5}$$

$$H_s(f) = \frac{Q_6}{Q_5}\cdot\sqrt{\frac{f^4Q_5^2+f^2f_5^2\left(1-2Q_5^2\right)+f_5^4Q_5^2}{f^4Q_5^2+f^2f_5^2\left(1-2Q_5^2\right)+f_6^4Q_6^2}} (H_s(f) = 1 for W_d) \tag{6}$$

$$H(f) = H_h(f)\cdot H_l(f)\cdot H_t(f)\cdot H_s(f) \tag{7}$$

Therefore, the weighted acceleration acting along the IMU's reference axis $j \in J$ can be obtained in the frequency domain, by multiplying $A_{ij}(f)$ by the total transfer function as follows.

$$Aw_{ij}(f) = A_{ij}(f)\cdot H(f) \qquad [m/s^2] \tag{8}$$

Subsequently, according to the well know Parseval's theorem, the weighted RMS calculation in time domain (Eq. (2)) can be replaced by the equivalent, and more straightforward, calculation in the frequency domain (Eq. (11)), where $\bar{r}_i$ and f_{ir} are computed as in Eq. (9) and in Eq. (10) respectively, and where the transition from the integral to the summation is due to the approximation introduced by the sampling discretisation.

$$\bar{r}_i = \frac{|U_i|}{2} + 1 \tag{9}$$

$$f_{ir} = \frac{r}{T_i}\,[Hz] \tag{10}$$

$$RMS_{aw_{ij}} = \left(\frac{1}{2}\cdot\int_0^{\frac{f_s}{2}} Aw_{ij}(f)df\right)^{\frac{1}{2}} \approx \left(\frac{1}{2}\cdot\sum_{r=1}^{\bar{r}_i} Aw_{ij}(f_{ir})\right)^{\frac{1}{2}} \quad \left[m/s^2\right] \quad \forall i \in I \quad \forall j \in J \tag{11}$$

STEP 3: Artificial Neural Network (ANN) training

STEP 3 trains an ANN to obtain a deterministic computation model that links the causes (i.e., the trial's explanatory factors) with their observed effects (i.e., the weighted RMSs). Training the ANN is an essential step because this network is the mathematical tool that will be used for the subsequent generation of simulated data through the MCS method described in STEP 4. Indeed, MCS is a numerical experimentation method to obtain the statistics of the output variables of a computational model, given the statistics of the input variables. Then, a numerical computation model is required. The ANN accomplishes this need by learning the laws that have produced the vibrational behaviour observed in the experimental trials, where the associated explanatory factor values are known, and building up a computation model. Then, the obtained computation model can be exploited to generate simulated data when simulated explanatory factor values will be provided by MCS. The choice of using an ANN is motivated by its higher predictive performance and its higher capacity for modelling non-linear phenomena if compared with more traditional tools, such as multiple regression models.

More formally, let:

- $\bar{\bar{I}} = \bar{\bar{E}}_{obs} \in \mathbb{R}^{|I|,|M|}$ be the input matrix for the ANN fitting process, i.e., the matrix of the explanatory variables observed during the set of experimental trials I.
- $\bar{\bar{T}} = \left[RMS_{aw_{ix}} RMS_{aw_{iy}} RMS_{aw_{iz}}\right] \in R^{|I|,3}(\forall i \in I)\left[m/s^2\right]$ be the target matrix for the ANN fitting process, i.e., the matrix of the acceleration weighted RMSs observed during the set of experimental trials I.
- $\bar{\bar{R}} \in \mathbb{R}^{|I|,3}\left[m/s^2\right]$ the residual matrix, i.e., the difference between the target matrix and those predicted by ANN.
- f be a mathematical function, which relates the input matrix $\bar{\bar{I}}$ to the target matrix $\bar{\bar{T}}$;
- g be an approximation of the function f;
- $\bar{\bar{\theta}}$ be the generic vector of the ANN parameters and $\bar{\bar{\theta}}_0$ the specific solution obtained through the learning phase.
- P be the set of ANN hidden layer perceptrons[2] and $p \in P$ be the generic perceptron.
- $Tr \subset I$, $Va \subset I$ and $Te \subset I$ be the ANN training, validation, and test set of trials, respectively.
- *RSS* be the Residual Sum of Squares, i.e., the sum of the squared differences between the observed and the predicted weighted *RMSs*.

Then, let's assume the existence of a mathematical function f which relates the input matrix $\bar{\bar{I}}$ to the target matrix $\bar{\bar{T}}$, such that $\bar{\bar{T}} = f\left(\bar{\bar{I}}\right)$. It can be interpreted as a deterministic computation model that links the causes ($\bar{\bar{I}}$) with their observed effects ($\bar{\bar{T}}$). The ANN defines a mapping $\bar{\bar{T}} = g\left(\bar{\bar{I}}, \bar{\bar{\theta}}\right) + \bar{\bar{R}}$ and learns the value of the parameter vector $\bar{\bar{\theta}}$ that results in the best approximation. To perform this mapping, a two-layer feed-forward network can be chosen as a first attempt, which is the more straightforward of the ANN architectures (MathWorks, 2022; Schmidhuber, 2015). Indeed, according to the parsimony principle, a simpler model with fewer parameters should be favoured over more complex models with more parameters, provided that the models fit the data well in a similar manner (e.g., Ventura et al., 2023). This is aimed at avoiding unnecessary complications that would make the model more resource-consuming to train and more difficult to read. In two-layer feed-forward networks, the information moves only in the forward direction from the input nodes, across the hidden nodes and towards the output nodes. This network is constituted of two layers of perceptrons: a hidden layer of $|P|$ perceptrons and an output layer on one perceptron. During the training phase, the ANN parameters are adjusted to minimise the *RSS*. To perform the training phase, the set of experimental trials (I) should be randomly split into three subsets: training, validation, and testing. The training set (Tr) is presented to the network during training, and the network is adjusted according to its error. The validation set (Va) is used to measure the generalization of the network and to stop training when generalisation stops improving, to prevent the overfitting phenomenon. The testing set (Te) has no effect on training and so

[2] A perceptron is the basic structure of the network and is a simplified model of a biological neuron.

provides an independent measure of network performance during and after training. Different training algorithms can be adopted, such as Levenberg-Marquardt, Bayesian Regularisation and Scaled Conjugate Gradient. For all these algorithms, the training procedure stops automatically at epoch in which the *RSS* on the validation set begins to increase, i.e., at the point beyond which the phenomenon of overfitting begins. At the end of the learning phase, the best parameter vector ($\overline{\overline{\theta}}_0$) is determined. It is noteworthy that training multiple times will generate different results due to different initial conditions and to the random set splitting.

STEP 4: Monte Carlo Simulation (MCS)

STEP 4 accounts for statistical uncertainty. Ideally, the uncertainty should be quantified by relying on a big experimental dataset. However, as the e-kick scoter is still a relatively emerging vehicle, the set experimental trials (I) acquired in STEP 1 may consist of only a few observations. Consequently, it should be replaced with a larger set of simulated trials (S) to enlarge the sample. According to STEP 4, simulated trials are generated applying the MCS technique that exploits the ANN computation model fitted in STEP 3.

Let:

- S be the set of simulated trials and $s \in S$ be the generic simulated trial.
- e_{sm} be the simulated value of the m^{th} explanatory variable (e_m) for the trial $s \in S$.
- $n_{sm} \in [0;1]$ be the random number associated with the explanatory variable value e_{sm}.
- F_m be the cumulative probability distribution function of the m^{th} explanatory variable.
- $\overline{\overline{E}}_{simul} = \left[e_{s1} e_{s2} \cdots e_{sm} \cdots e_{s|M|}\right] \quad \in R^{|S|,|M|} \quad (\forall s \in S; \forall m \in M)$ be the matrix of the simulated explanatory variables for the set of simulated trials S.
- $RMS_{aw_{sj}}$ be the simulated weighted RMS associated with acceleration acting along the IMU's reference axis $j \in J$ during the simulated trial $s \in S$.
- $R\overline{\overline{M}}S_{simul} = \left[RMS_{aw_{sx}} RMS_{aw_{sy}} RMS_{aw_{sz}}\right] \quad \in R^{|S|,3} \quad (\forall s \in S) \quad \left[m/s^2\right]$ be the matrix of the simulated weighted RMSs for the set of simulated trials S.

In MCS, each trial explanatory variable e_m is interpreted as a random variable and then an appropriate cumulative distribution function (F_m) is assumed. This distribution must be carefully defined to ensure a realistic description of the existing boundary conditions in the experimental trials and, thus, guarantee reliable simulated data. Indeed, the cumulative distribution functions of the trial explanatory variables will have strong implications for the subsequent statistical analysis and may introduce bias if they are not reliable. In the specific case, the distributions associated with the users' characteristics, such as gender, age, height, and mass, can be found from the literature. The distributions associated with surface typology, vehicle typology and sensor position could be assumed as uniformly distributed to obtain equal sized simulated trial subsets reflecting that already done in the experimental trials. This is aimed at facilitating the interpretation of the results. Finally, the distribution associated with the travel speed could be empirically constructed through a statistical analysis of the frequencies observed during the set of experimental trials (I) to replicate the trial boundary conditions. For each explanatory variable e_m and for each simulated trial $s \in S$, a random number (n_{sm}) should be generated through the extraction of a random variable uniformly distributed in the interval [0;1]. Then, the simulated value of the explanatory variable (e_{sm}) can be determined by inverting the associated distribution function according to Eq. (12).

$$e_{sm} = F_m^{-1}(n_{sm}) \qquad \forall s \in S \qquad \forall m \in M \tag{12}$$

Collecting the simulated values for each explanatory variable e_m and for each simulated trial $s \in S$, the matrix of the simulated explanatory variables ($\overline{\overline{E}}_{sim}$) is then obtained. Applying the deterministic computational model (i.e., the ANN trained in STEP 3, mathematically defined by the function g and the parameter vector $\overline{\overline{\theta}}_0$) to the matrix of the simulated explanatory variables, then the corresponding matrix of the simulated weighted RMSs ($R\overline{\overline{M}}S$*accordingtoEq.*(13).

$$R\overline{\overline{M}}S_{simul} = g\left(\overline{\overline{E}}_{simul}, \overline{\overline{\theta}}_0\right) \qquad \left[m/s^2\right] \tag{13}$$

Hence, the observed (deterministic) model is turned into a stochastic model.

STEP 5: Simulated weighted RMS vibration total value computation

Next, according to STEP 5, the simulated vibration total value is computed. This is a synthetic vibration index aiming to globally characterize the solicitation acting on the vehicles.

More formally, let:

- k_j be the multiplying factor associated with acceleration acting along the IMU's reference axis $j \in J$.
- RMS_{aw_s} be the simulated vibration total value of the weighted RMS acceleration acting during the simulated trial $s \in S$.

The simulated weighted $RMS_{aw_{sj}}$ associated with the accelerations acting along the three orthogonal axes ($\forall j \in J$), for the set of simulated trials ($\forall s \in S$), computed as described in STEP 4, should be combined adopting three multiplying factors (k_x,

k_y, k_z) to obtain the simulated weighted vibration total value (RMS_{aw_s}) (Eq. (14)). In the case of the human sensitivity to whole-body vibrations, that can affect the comfort on a ride, the multiplying factors can all be assumed equal to 1 for both a seated and a standing person (ISO, 1997). Therefore, RMS_{aw_s} coincides with the Euclidean norm of the RMS vector.

$$RMS_{aw_s} = \left(k_x^2 RMS_{aw_{sx}}^2 + k_y^2 RMS_{aw_{sy}}^2 + k_z^2 RMS_{aw_{sz}}^2\right)^{\frac{1}{2}} \ [m/s^2] \forall s \in S \tag{14}$$

STEP 6: Statistical Z-test on the pavement surface typologies

Afterwards, according to STEP 6, the average vibration total values acting on the e-kick scooter and on the e-bike are computed and tested by the statistical Z-test, to discover if significant differences exist among the trials performed on the two vehicles, for each pavement surface.

More formally, let:

- B be the set of surface typologies and $\beta \in$ B be the generic surface typology (e.g., uneven cobblestone).
- V be the set of vehicles and $v \in V$ be the generic vehicle typology (i.e., *ekick* or *ebike*).
- z_β be the z value associated with RMS_{aw_s} averages for the simulated trials performed on surface typology β.
- α be the significance level for the statistical Z-test.
- z_{crit} be the critical value for the z variable, i.e. the z value associated with the significance level (α) adopted for the two tailed tests.

If the observed z value (z_β) is greater than z_{crit} or smaller than $-z_{crit}$, then the null hypothesis can be rejected (Eq. (15). Thus, the alternative hypothesis that there is a statistical difference between the average vibration total values acting on the two vehicles $v \in V$ is accepted. This means that e-kick scooter and e-bike behave differently during the simulated trials conducted on surface typology $\beta \in$ B. Otherwise, the null hypothesis cannot be rejected, and the two vehicles have a similar vibrational behaviour on the considered pavement typology.

Formally:

$$\begin{cases} \text{If } |z_\beta| > z_{crit} \\ \text{then} \\ \text{The average RMS acting on the two vehicles differs for the surface typology } \beta \in \text{B} \\ \text{otherwise} \\ \text{The average RMS acting on the two vehicles is equal for the surface typology } \beta \in \text{B} \end{cases} \tag{15}$$

STEP 7: Multiple Linear Regression (MLR) models

Next, several MLR models are developed to understand which factors affect the vibrational magnitude and their extent for each vehicle, respectively. Indeed, although at first glance the ANN and MLR models may appear to accomplish the same tasks, they serve different needs, namely prediction performance the former, and the ability to understand the effect of each explanatory factor on the vibrational magnitude level the latter (Alqatawna et al., 2021; Zhang, 2010).[3]

On the one hand, if the null hypothesis of the Z-test cannot be rejected for all pavement surfaces ($|z_\beta| \leq z_{crit} \ \forall \beta \in B$), then there is not a statistically significant difference between the vibrational responses associated with the two vehicles. Therefore, a single global MLR model is enough to explore the effects affecting the vibrational magnitude of e-kick scooter and e-bike, respectively. On the other hand, if the null hypothesis of the Z-test can be rejected for at least one pavement surface ($\exists \beta \in B : |z_\beta| > z_{crit}$), then there is a significant difference between the vibrational responses associated with the two vehicles. Hence, two separate MLR models should be estimated, one for each vehicle, respectively. For both cases, once the models have been estimated, they should be evaluated by analysing the goodness-of-fit statistics and the values of the regression coefficients, to understand the influence that the explanatory variables could have on the vibrational behaviour of the two vehicles.

More formally, let us assume the simulated weighted RMS vibration total value as the dependent variable of the MLR model and let:

- V be the set of vehicles and $v \in V$ be the generic vehicle typology (i.e., *ekick* or *ebike*).
- m_v the index of the independent variable associated with the vehicle typology.
- $S_v \subset S$ be the subset of the simulated trials performed on the vehicle $v \in V$.
- RMS_{aw_s} be the observed value of the response variable for simulated trial $s \in S$.
- $\widehat{RMS_{aw_s}}$ be the predicted value of the response variable for simulated trial $s \in S$.

[3] Compared to MLRs, ANN models offer advantages and disadvantages. On the one hand, ANNs have a larger potential for modelling non-linear processes, which generally leads to a superior prediction performance (Alqatawna et al., 2021). Additionally, ANNs do not require assumptions about an underlying relationship between the predictors and the observed vibrational magnitudes. They could also handle predictor correlation issues more effectively than MLRs. On the other hand, ANNs are "black box" models. Black box models are functional relationships between system inputs and system outputs, and the parameters of these functions have no real-world meaning (Zhang, 2010). Consequently, it is challenging to understand the effect that each predictor has on the response variable.

- b_0 and $b_{0\,v}$ be the constant of the regression (hyperplane intercept) for the global and for the vehicle $v \in V$ MLR model, respectively.
- b_m and $b_{m\,v}$ be the regression coefficient associated with the explanatory variable e_m for the global and for the vehicle $v \in V$ MLR model, respectively.
- p_m and $p_{m\,v}$ be the p-value associated with the explanatory variable e_m for the global and for the vehicle $v \in V$ MLR model, respectively.
- R^2_{adj} and $R^2_{adj\,v}$ be the adjusted R-squared associated with the global and the vehicle $v \in V$ MLR model, respectively.
- F and F_v be the F-value associated with the global F-test conducted on the global and on the vehicle $v \in V$ MLR model, respectively.

Specifically, if Eq. (16) is not satisfied, i.e.,

$$\exists \beta \in B : |z_\beta| > z_{crit} \tag{16}$$

Then, a single global Multiple Linear Regression (MLR) model could be run as shown in Eq. (17) for both vehicles simultaneously.

$$RMS_{aw_s} = b_0 + \sum_{m \in M} b_m e_{sm} \qquad \forall s \in S \tag{17}$$

Otherwise, two MLR vehicle-specific models need to be fitted according to Eq. (18).

$$RMS_{aw_s} = b_{0\,v} + \sum_{\substack{m \in M \\ (m \neq m_v)}} b_{m\,v} e_{sm} \quad \forall s \in S_v \qquad \forall v \in V \tag{18}$$

The ordinary least squares method can be used to estimate the best possible coefficients of the MLR models. Once the models have been estimated, they could be evaluated by the following goodness-of-fit statistics: the R^2_{adj} (or $R^2_{adj\,v}$) and the linear correlation between predictors and the response variable, indicated by the global F-test and the corresponding significance value F (or F_v). The value of the coefficient b_m (or $b_{m\,v}$) and their significance value p_m (or $p_{m\,v}$) should also be evaluated to understand the influence that explanatory variable e_m could have on the vibrational behaviour of the two vehicles.

4. Real world experiment

4.1. Research context

The proposed framework was experimented in a real Italian case study. Urban roads were considered in this research, as the urban environment is the one with the greatest presence of micromobility users. Precisely, experimental trials were carried out using two vehicles on five different urban paths located in the city of Brescia (Lombardy Region), which is one of the most important industrial, commercial, and social hubs in Italy (De Aloe et al., 2022; Martinelli et al., 2022).

The two vehicles (see Fig. 2) were an e-bike (city bike, 26″ pneumatic tyres, 26.9 kg mass, front and rear V-brakes) and an e-kick scooter (aluminium frame, 10″ pneumatic tyres, 14.2 kg mass, front electric brakes, and rear disc brakes). These specific vehicles were adopted as they exhibited average characteristics compared to the European market. Therefore, they were considered representative of the e-PMVs most used on European urban patterns.

The five paths (see Fig. 3) were characterised by different surfaces, with diverse levels of irregularity, such as bituminous conglomerate, uneven cobblestone, regular cobblestone, metal ventilation grids and alternated dirt and concrete road.

Table 3 reports a summary of the characteristics of the paths tested.

As for the path lengths, the typical journeys made by e-kick scooter and e-bike users were considered according to Zagorskas and Burinskienė (2020). Therefore, considering the characteristics of the city routes and public spaces, the test path lengths ranged from a minimum of 710 m to a maximum of 1,155 m. Grids were an exception, because this type of surface can be treated as a possible variation of other types of paths. Indeed, grids were analysed separately to have a better homogeneity of the chosen paths, taking advantage of a case of large grids extensively available in the city centre.

For this study, six volunteers (3 males and 3 females) with the same level of expertise (beginner) with e-bikes and e-kick scooters were chosen among the staff of Brescia University to ensure a certain variability in term of age, mass, and height. Moreover, the selected age range (i.e., 23 to 35 years old) is the most common among e-bikes and e-kick scooter users, according to Boglietti et al. (2021). Table 4 provides a summary of the characteristics of the six volunteers.

Volunteers were instructed to move along the path at predetermined speeds to ensure consistency between the different trials. The test was repeated at two different speeds (10 km/h and 15 km/h) to assess the impact of riding speed on comfort. In the case of uneven cobblestones, maintaining the speed of 15 km/h was not possible owing to the excessive stress and difficulty perceived by users. The travel speeds were shown by a digital tachometer installed on the vehicles. During the trials, experimentation assistants made sure there were no obstacles (people, other vehicles, objects, etc.) along the paths. All the tests were conducted in the daytime, in fair weather, and on dry surfaces.

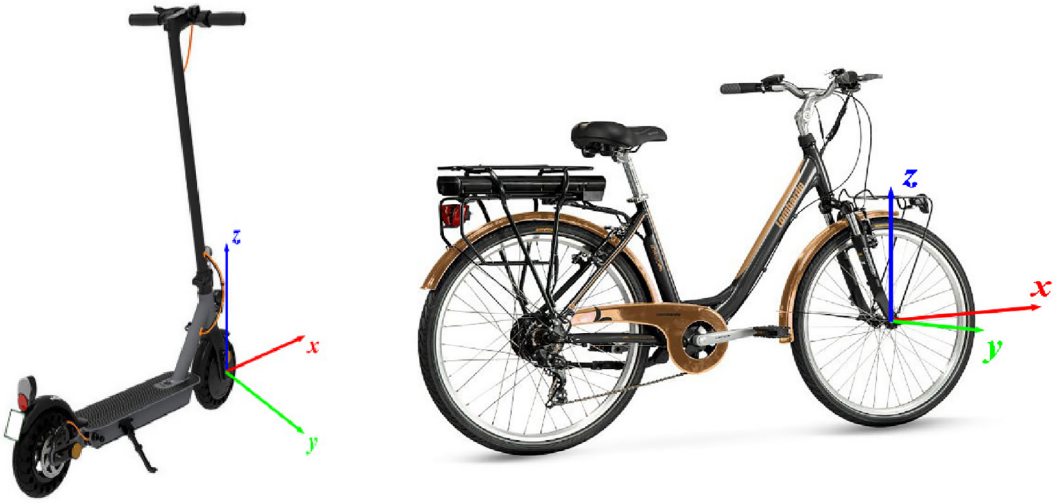

Fig. 2. The e-bike and the e-kick scooter used in the study.

Fig. 3. Surface types, from left to right: bituminous conglomerate, uneven cobblestone, regular cobblestone, metal ventilation grid, and alternated dirt and concrete road.

Table 3
Path's characteristics.

Path ID	Pavement surface	Path description	Length [m]	Travel speed [km/h]
A	Uneven cobblestone	Three laps around a square	800: Total *(266.7: Each lap)*	10: Each lap
C	Bituminous conglomerate	Round trip along a cycle path	800: Total *(400: Way out)* *(400: Way back)*	10: Way out15: Way back
G	Metal ventilation grids	Two closed laps on the grids placed in a square.	355: Total *(177.5: Each lap)*	10: First lap15: Second lap
P	Regular cobblestone	Round trip around a square	Total: 710 *(380: Way out)* *(330: Way back)*	10: *Way out* 15: *Way back*
S	Alternated dirt and concrete road	Two laps around a closed cycle path	1,155: Total *(577.5: Each lap)*	10: First lap15: Second lap

Table 4
User's characteristics.

User ID	Gender	Age [year]	Height [m]	Mass [kg]
1	Male	29	1.86	87
2	Male	27	1.80	72
3	Female	35	1.63	79
4	Female	23	1.61	50
5	Male	27	1.84	80
6	Female	29	1.78	60

Kinematic measurements were made with two IMUs mounted on vehicle bodies and equipped with accelerometer, gyroscope, and inclinometer sensors. The IMUs were fixed to the e-bike and e-kick scooter handlebars (front position), as well as the e-bike rear rack and e-kick scooter platform (rear position). The sensors have always been kept in a horizontal position, so that the IMU's x axis was parallel to the vehicle's longitudinal axis, its y axis was parallel to the vehicle's transversal axis, and its z axis was parallel to the vehicle's vertical axis. During each trial, raw acceleration data were collected for the three IMU reference axes, real time broadcasted through Bluetooth connection to a smartphone carried by the users and saved in CSV files.

4.2. Application of the proposed framework

A set of explanatory variables ($e_m \ \forall m \in M$) was defined according to STEP 1, to ensure a viable description of the trial boundary conditions. These variables are illustrated in Table 5, which is self-explicative and reports descriptive statistics. Some variables are continuous, while some others are categorical and are coded as binary for modelling purposes. A set of 168 experimental trials (I) was performed: 80 trials were related to the e-bike and 88 trials were related to the e-kick scooter. Adopting a sampling frequency (f_s) of 200 Hz, the accelerometric data ($a_{ij}(t)$) were acquired at the sampling times defined in Eq. (1). Next, according to STEP 2, the ISO 2631–1 basic vibration evaluation method was applied for the computation of the weighted RMS ($RMS_{aw_{ij}}$) acting along the three IMUs' reference axes $j \in J$ during each trial $i \in I$. The digital filters for the total transfer function for health and comfort ($H(f)$) were defined from Eq. (3) to Eq. (8). Using Eq. (9), Eq. (10) and Eq. (11), a total of 504 RMS values were then computed.

Next, according to STEP 3, a two-layer feed-forward ANN was trained adopting the Matlab® Neural Net Fitting Tool, to create a deterministic computation model that links the trial explanatory variables ($\bar{\bar{E}}_{obs}$) with the corresponding observed weighted RMSs ($RMS_{aw_{ij}}$). To perform the training of the network, the set of experimental trials was randomly split into training (Tr), validation (Va), and testing subsets (Te), consisting of 70 %, 15 % and 15 % of the total observations, respectively (e.g., Flach, 2012). In addition, these percentages provide a large training set while ensuring enough observations for validation and testing procedures. Numerous attempts of enhancement were achieved by tuning the number of perceptrons in the hidden layer and the training algorithm. As a result, a network with 10 perceptrons in the hidden layer and trained with the Levenberg-Marquardt algorithm was chosen as the final model because it outperformed all other configurations. Fig. 4 supported the high predictive capacity of the selected ANN, since the R statistic was close to 1 both for the training and validation subsets, and for the testing subset.[4] Particularly, the last result was fundamental because the testing subset did not affect the training process and then provided an unbiased endorsement of network performance in predicting unseen data. Moreover, this was a prerequisite for the subsequent generation of simulated data through the MCS technique. Indeed, it guaranteed that the data generated by the simulation will be as those obtained by running real trials. Furthermore, the R statistic close to 1 demonstrated that more complex ANN architectures (such as those with more than two layers) were an unneeded complication that would have increased the model's resource requirements for training and reading without significantly enhancing its predictive power. Hence, the parsimony principle was supported.

Next, according to STEP 4, a cumulative distribution function (F_m) was defined for each trial explanatory variable (e_m), as shown in Table 6. The distributions associated with the users' characteristics were defined drawing from literature data concerning the population characteristics (Istat, 2021; Lundh, 2009). The considered ages ranged between 20 and 40 years, to ensure consistency with the sample investigated during the experimental trials. The pavement surface typology, vehicle typology and the sensor position were assumed uniformly distributed. This was aimed at obtaining an equal size simulation subset for the different categories of these variables to make the data interpretation more straightforward. Finally, the travel speed was assumed normally distributed and the parameters (i.e., mean, and standard deviation) were empirically determined analysing the set of experimental trials.

Subsequently, the simulated values of the explanatory variables (e_{sm}) were determined by inverting the associated distribution functions as indicated in Eq. (12). Applying the Eq. (13), the matrix of the simulated independent variables ($\bar{\bar{E}}_{sim}$) was then generated for a set (S) of 10′000 simulated trials. Adopting the ANN model trained in the previous step, the matrix of the simulated weighted RMS ($\bar{\bar{RMS}}_{simul}$) was consequently generated, for a total of 30′000 values (i.e., an RMS value for each of the three IMUs' reference axes during each of the 10′000 simulated trials).

Afterwards, according to STEP 5, the accelerations along the three orthogonal axes were combined adopting three unitary multiplying factors (k_x, k_y, k_z) as indicated in Eq. (14) to obtain the simulated weighted RMS vibration total value (RMS_{aw_s}). A set of 10′000 vibration total values were then generated, i.e., an RMS value for each of the 10′000 simulated trials.

4.3. Results and discussion

According to STEP 6, the differences between the average simulated vibration total values RMS acting on the two vehicles were tested through the statistical Z-test (Eq. (15)), to discover if significant differences exist, for each pavement surface. The results are shown in Table 7.

[4] Noteworthy, the closer to 1 is R, the greater is the model performance, since R=1 indicates a perfect correlation between observed and predicted values.

Table 5
Summary characteristics for the experimental trial independent variables.

Trial explanatory variable	Symbol	Unit of measure	Type	Data source	Min.	Max.	Mean	Std. Dev.
Surface typology								
Contrast = Bituminous conglomerate (C)								
Uneven cobblestone (A)	e_1	[-]	Binary	OFO	0	1	0.14	0.35
Metal ventilation grids (G)	e_2	[-]	Binary	OFO	0	1	0.25	0.43
Regular cobblestone (P)	e_3	[-]	Binary	OFO	0	1	0.14	0.03
Alternated dirt and concrete road (S)	e_4	[-]	Binary	OFO	0	1	0.24	0.43
Vehicle typology								
Contrast = E-bike (ebike)								
E-kick scooter (ekick)	e_5	[-]	Binary	OFO	0	1	0.52	0.50
Sensor position								
Contrast = Front (F)								
Rear (R)	e_6	[-]	Binary	OFO	0	1	0.52	0.5
Travel speed	e_7	[km/h]	Continuous	DM	10.00	15.00	12.14	2.29
User gender								
Contrast = Male (Ma)								
Female (Fe)	e_8	[-]	Binary	OFO	0	1	0.46	0.50
User age	e_9	[year]	Continuous	OFO	23.00	35.00	28.93	3.37
User height	e_{10}	[m]	Continuous	DM	1.61	1.86	1.77	0.09
User mass	e_{11}	[kg]	Continuous	DM	50.00	87.00	73.23	11.28

DM = Direct Measure; OFO = On the Field Observation.

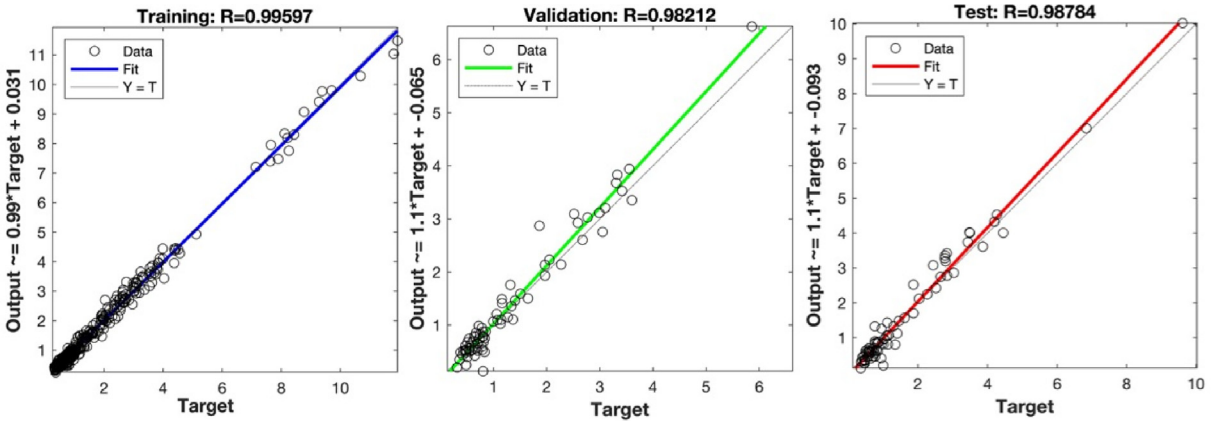

Fig. 4. ANN regression charts for training subset, validation subset, testing subset and all trials set.

Consistent with a general perspective, the e-kick scooter presents higher vibrations than the e-bike for each pavement surface. Indeed, for all surfaces (β), the Z-test showed that the differences between the means were statistically significant at the 5 % significance level. More specifically, the mean weighted accelerations acting on the e-kick scooter resulted higher than those acting on the e-bike. As a result, the e-kick scooter appeared to be less comfortable than the e-bike. The distinct technical and structural properties of the e-kick scooter (e.g., smaller wheels, stiffer frame, smaller damping factor) could explain its observed lesser comfortability. As for the e-kick scooter, the highest mean weighted acceleration was recorded on the uneven cobblestone (A), while the lowest mean weighted acceleration was recorded on surface C. As for the e-bike, the highest mean weighted acceleration was recorded on surface A, while the lowest mean weighted acceleration was recorded on surface G. As expected, the uneven cobblestone surface (A) induced much stronger vibrational accelerations than other surfaces for both vehicles. In opposition, the most comfortable surface for the e-kick scooter appeared to be the bituminous conglomerate (C), while the metal ventilation grids (G) emerged to be the least soliciting for the e-bike. This diverse behaviour could be explained by the different ratio between the characteristic dimension of the wheel and the characteristic dimension of the surface irregularity. From a practical perspective, these results indicated that the uneven cobblestone surface should be avoided for both vehicles when planning a path. This recommendation acquires even greater importance for the e-kick scooter, being the vehicle that is most solicited by the irregularities of this surface. This could be a challenging issue for the paths located the historical city centres, where the uneven cobblestone is a widespread pavement surface. Conversely, the bituminous conglomerate could be considered the best surface typology for both the vehicles, with the metal ventilation grids indicating elements unsuitable to be chosen as a pavement solution for long stretches. The observed lower e-kick scooter comfort is consistent with recent research (Boglietti et al., 2022). However, they observed that

Table 6
Summary for the simulated trial independent variables distributions.

Trial independent variable	Symbol	Distribution	Data source	Mean	Std. Dev.
Surface typology					
Contrast = Bituminous conglomerate (C)					
Uneven cobblestone (A)	F_1	Uniform	[-]	[-]	[-]
Metal ventilation grids (G)	F_2	Uniform	[-]	[-]	[-]
Regular cobblestone (P)	F_3	Uniform	[-]	[-]	[-]
Alternated dirt and concrete road (S)	F_4	Uniform	[-]	[-]	[-]
Vehicle typology					
Contrast = E-bike (ebike)					
E-kick scooter (ekick)	F_5	Uniform	[-]	[-]	[-]
Sensor position					
Contrast = Front (F)					
Rear (R)	F_6	Uniform	[]	[-]	[-]
Travel speed	F_7	Normal	ETA	12.10 km/h	2.30 km/h
User gender					
Contrast = Male (Ma)					
Female (Fe)	F_8	Empirical[1]	L (Istat, 2021)	[-]	[-]
User age	F_9	Empirical[1]	L (Istat, 2021)	[-]	[-]
User height	F_{10}	Normal	L (Lundh, 2009)	1.78 m (male) 1.65 m (female)	0.062 m (male) 0.055 m (female)
User mass	F_{11}	Normal	L (Lundh, 2009)	73.80 kg (male) 61.50 kg (female)	9.80 kg (male) 10.50 kg (female)

L = Literature; ETA = Experimental Trials Analysis.
[1] Only the subjects aged between 20 and 40 years were considered.

Table 7
Results of the Z-test concerning the average simulated vibration total values (RMS_{aw}) computed for the different pavement surfaces (β) and for the two vehicles (v). The z_{crit} associated with the 5% significance level is 1.96.

Pavement surface ($\boldsymbol{\beta}$)	E-kick scooter ($\boldsymbol{v} = \boldsymbol{ekick}$)		E-bike ($\boldsymbol{v} = \boldsymbol{ebike}$)		Z - test	
	Mean $[\boldsymbol{m}/\boldsymbol{s}^2]$	Variance $[\boldsymbol{m}^2/\boldsymbol{s}^4]$	Mean $[\boldsymbol{m}/\boldsymbol{s}^2]$	Variance $[\boldsymbol{m}^2/\boldsymbol{s}^4]$	$z_{y_{s_\beta}}$	Can be H_0 rejected?
A	8.31	0.86	7.24	9.46	10.45	Yes
C	2.62	0.59	1.91	1.36	15.99	Yes
G	2.82	0.49	1.47	0.43	44.03	Yes
P	3.72	0.37	2.67	1.91	22.23	Yes
S	3.37	0.85	2.41	2.03	18.13	Yes
All	4.19	5.07	3.14	7.35	21.11	Yes

the means of the vibrational magnitudes were not statistically significantly different for the uneven cobblestone surface (A). This different outcome could be explained by having analysed only a small sample of experimental trials.

Table 7 also shows the null hypothesis of the Z-test is rejected for all pavement surfaces. Therefore, as suggested by Eq. (16), two separate MLR models (Eq. (18)) were estimated for the two vehicles, according to STEP 7. The results are shown in Table 8, where the numerical entries in bold represent significant variables at <0.05 level. As a general perspective, both the MLR models overall had a good fit and can explain a significant amount of the observed deviances from the means. The best predictive performance was associated with the e-kick scooter model. Almost all the explanatory variables resulted highly significant ($p_{m\,v} \ll \alpha = 0.05$). These significance values, higher than those obtained by Boglietti et al. (2022), constitute an improvement on the previous work. This improvement has been made possible by the expansion of a set of experimental data with a large set of simulated data generated by applying the ANN tool and MCS technique.

Focusing on each explanatory variable separately, the following considerations result.

As for the pavement surface, the findings show that this factor has a highly significant effect on the vibrational magnitude, in accordance with the literature (Bíl et al., 2015; Chou et al., 2015; Gao et al., 2019; Cano-Moreno et al., 2021). Particularly, the positive signs indicated that uneven cobblestone (A), regular cobblestone (P) and alternated dirt and concrete road (S) surfaces induced higher vibrational magnitudes than the bituminous conglomerate (C) for both the vehicles. On the contrary, the metal ventilation grids (G) surface had a contrasting effect on the vehicles. Indeed, on the one hand, a positive sign was obtained for the e-kick scooter model, meaning that this surface was less comfortable than bituminous conglomerate. On the other hand, a negative sign was found for the e-bike model, meaning that this surface was more comfortable than the bituminous conglomerate. This is consistent with what was observed in the Z-test and could still be explained by the different ratio between the characteristic dimension of the wheel and the characteristic dimension of the surface irregularity. These results corroborate Boglietti et al. (2022), although the significances of the regression coefficients have been remarkably

Table 8
Vehicle specific MLR models for the prediction of the simulated weighted RMS vibration total value (RMS_{aw}).

Explanatory variables		E-kick scooter model ($v = ekick$)				E-bike model ($v = ebike$)			
Trial explanatory variable	**Symbol**	**Estim. (b_{mv})**	**p-val (p_{mv})**	**Low. 95 %**	**Upp. 95 %**	**Estim. (b_{mv})**	**p-val (p_{mv})**	**Low. 95 %**	**Upp. 95 %**
Hyperplane intercept	[]	1.040	**<0.001**	0.483	1.598	2.096	**<0.001**	1.149	3.043
Pavement surface									
Contrast = Bituminous conglomerate (C)									
Uneven cobblestone (A)	e_1	5.671	**<0.001**	5.615	5.726	5.335	**<0.001**	5.241	5.429
Metal ventilation grids (G)	e_2	0.174	**<0.001**	0.118	0.229	−0.436	**<0.001**	−0.530	−0.341
Regular cobblestone (P)	e_3	1.081	**<0.001**	1.026	1.136	0.723	**<0.001**	0.629	0.816
Alternated dirt and concrete road (S)	e_4	0.746	**<0.001**	0.690	0.802	0.540	**<0.001**	0.448	0.633
Sensor position									
Contrast = Front (F)									
Rear (R)	e_6	0.035	**<0.001**	0.001	0.070	2.558	**<0.001**	2.499	2.617
Travel speed	e_7	0.110	**<0.001**	0.102	0.117	0.078	**<0.001**	0.065	0.090
User gender									
Contrast = Male (Ma)									
Female (Fe)	e_8	0.536	**<0.001**	0.480	0.592	0.503	**<0.001**	0.408	0.598
User age	e_9	−0.063	**<0.001**	−0.066	−0.060	−0.068	**<0.001**	−0.073	−0.063
User height	e_{10}	0.768	**<0.001**	0.471	1.065	−0.644	0.013	−1.152	−0.137
User mass	e_{11}	0.009	**<0.001**	0.007	0.011	0.007	**<0.001**	0.004	0.010

E-kick scooter model ($v = ekick$): 4′981 observations, $R^2_{adj\,v} = 0.92$, $F_v = 5998.9$.
E-bike model ($v = ebike$): 5′019 observations, $R^2_{adj\,v} = 0.85$, $F_v = 2751.7$.

improved thanks to the simulation. From a practical viewpoint, the evidence confirms that the bituminous conglomerate could be considered the best surface typology for both the vehicles when planning a new path.

As for the sensor position, the coefficient closest to zero of the e-kick scooter model indicates that rear and front position have a similar vibration total value for this vehicle. Conversely, the positive sign of the e-bike regression model suggests that in this case the rear position records a greater vibration total value. This high solicitation difference between rear and front position is explained by the e-bike front wheel damping device, that attenuates the shocks due to the pavement surface irregularities and thus provide a greater comfortability.

As for travel speed, the positive signs indicate that an increase of this variable implies an increase of the vibrational magnitude, consistent with the findings of Bíl et al. (2015). In particular, the highest coefficient is obtained for the e-kick scooter regression model, suggesting the greater effect that the travel speed has on the vibration total value acting on this vehicle. Also, in this case the solicitation difference could be explained by the e-bike front suspension, which has a non-linear behaviour that results in greater absorption of vibrations of greater magnitude, as suggested by Cano-Moreno et al. (2021) in the hypothesis of the flexible suspension e-scooter. This evidence has significant concrete implications, as they suggest the need to enhance the e-kick scooter design by equipping them with shock absorbers.

As for the user gender, the positive coefficients indicated that the females experienced a higher vibration magnitude for both vehicles maybe due to a different physical characteristic or followed trajectory. Indeed, the paths were characterised by a certain width (about 2 to 3 m). Consequently, different trajectories were possible along the same fixed path. Thus, more cautious users could have avoided some irregularities in the pavements on the contrary than less prudent ones. On the other hand, this result suggests that females could tend to feel more uncomfortable and insecure when using e-PMVs and confirms the negative propensity of female users toward micromobility (Azimi et al., 2021). Moreover, this result might justify why females are more prone than males to an injury outcome from e-kick scooter's crashes (Tian et al., 2022). Indeed, although empirical evidence is not yet available, the greater solicitation acting on women, coupled with the small diameter of e-kick scooter's wheels, could occasionally lead to a loss of balance, and thus a greater likelihood of crashes due to falling from the vehicle. Nevertheless, new studies are recommended to clarify these issues.

As for the user age, the vibration total value appeared to reduce as the age increased for both vehicles. This could be explained by a more prudent behaviour of 'older' users.

As for the user height, a different comportment between the two vehicles was observed. Indeed, the vibrational magnitude acting on the e-kick scooter strongly increases with the height, while an opposite effect occurred on the e-bike. This contrasting evidence is a symptom of a different response between the two vehicles and could be explained by the different vehicle-rider scenarios (i.e., standing on the e-kick scooter and sitting on the e-bike). As a practical consequence, it suggests the need for a greater caution by taller users when riding e-kick scooters.

Finally, as for the user mass, the coefficients close to zero indicate that it had only a slight influence on the vibrational acceleration for both the vehicles. This is consistent with the well-known Newton's second law, according to which users with greater mass will have experienced equal accelerations but greater forces.

5. Conclusions

The proliferation of e-kick scooters in many cities worldwide has disrupted the transport sector and captured the attention of several stakeholders owing to the issuing of a few regulations to allow their circulation on roads. In this context, e-kick scooters were equated with e-bikes according to some European rules. However, because these vehicles do not have the same characteristics, this similarity could be questionable, at least in terms of dynamic behaviour. While the literature has investigated the dynamic behaviour of bikes, as far as the authors are aware, no previous experimental investigation has been conducted to compare the vibrational behaviour of e-kick scooters and bikes. Only one study provided a first attempt for this evaluation, nonetheless it adopted only a limited sample of real data without data expansion and further refinements.

Therefore, this paper contributes to the field in a fourfold manner, as follows:

- A novel framework for investigating and comparing the vibrational behaviour of e-bikes and e-kick scooters focusing on the vehicular reaction at pavement irregularities, travel speed and users' characteristics is proposed.
- This framework integrates the ISO 2631–1 vibration evaluation method, Artificial Neural Network, Monte Carlo Simulation and Multiple Linear Regression models.
- A full application of the practical effectiveness of this framework in a real environment taking the city of Brescia (Italy) as a case study is provided.
- An identification of the key factors that influence the magnitude of vibrations for e-scooters and e-bikes is performed. Particularly, statistical z-tests and MLR are applied to discover if there are any significant differences in the vibration levels acting on an e-kick scooter and an e-bike, as well as to verify which factors affect these vibration levels.

The empirical results indicated a significant difference between the vibrational behaviour of the two vehicles in all the analysed surfaces. Moreover, they provided evidence on the questionability of equating e-kick scooters and e-bikes when the vibrational performance is considered as comparative parameter. Indeed, the e-kick scooter's mean vibrational magnitudes were significantly greater than those acting on the e-bike. Consequently, the e-kick scooter appeared to be globally less comfortable than the e-bike. Furthermore, the MLR models demonstrated that not only the pavement surface and travel speed parameters contribute in distinct ways to the vibrational magnitude explanation for the two vehicles, but also sensor position (rear or front), user gender and user height.

This research has relevant practical implications for the vehicle design and planning. As for vehicle design, the results indicated that the main reason for the greater e-bike comfortability was due to the presence of the front shock absorber. This evidence suggests the need to improve the e-kick scooter fleets by equipping them with shock absorbers, as is already usual for the most widespread e-bike typologies.

As for a planning perspective, the outcomes indicated that the bituminous conglomerate could be considered as the best surface typology for both the vehicles when paths need to be identified. Furthermore, the uneven cobblestone should be avoided because it induces much stronger vibrational accelerations than other surfaces for both vehicles. This advice is even more important for the e-kick scooter, which is the vehicle that is most affected by the unevenness of this surface, and which could pose a safety risk. This could be an obstacle for routes in old city centres, where uneven cobblestone is a common pavement surface. Moreover, the results suggested the necessity of limiting the travel speed when riding e-kick scooters, especially for tall users, as the vibrational magnitude is strongly increased by the height factor.

Nevertheless, the main limitation of this research is the not very large scale of application. Indeed, only one e-kick scoter and one e-bike models were ridden in the experimental trials. In addition, the statistical uncertainty of the model is accounted through the assumptions of the probability distribution of the inputs in MCS. These assumptions could have significant effects on the consequent statistical analysis. Therefore, further data collection is recommended to corroborate the results by quantifying the model uncertainty based on larger real-world data samples. However, this study is sufficiently large to contribute to the research evidence base on this topic, because:

- The vehicles adopted for the experimental trials can be considered representative of the e-PMVs most used on European urban patterns, since they have average characteristics compared to the European market.
- The experimental data are expanded to include uncertainty by applying a MCS based on a two-layer feed-forward ANN.
- The probability distributions of MCS are carefully chosen to achieve simulation results characterized by a high level of realism.
- An explicit indication of key determinants affecting the vibrational magnitude acting on e-kick scooters and e-bikes is provided.
- The proposed methodology has general validity. Thus, providing new input data, it can be employed to any vehicular sample and to any driving context.

Finally, this study indicates several developments. Firstly, future research should deepen the differences in behaviour between the two vehicles, not only in terms of RMS vibration total value, but also by analysing the RMS associated with acceleration acting along the three IMUs' reference axis separately and the vehicular rotational motion (i.e., yaw, pitch, roll).

Secondly, only physical user's variables were considered in this research, because were assumed being those that directly influence the vehicle vibrational response. Hence, future studies may investigate other variables related to users, such as socio-demographic and behavioural ones (e.g., income level, educational level, job position, trip motivation, trip frequency). Indeed, since the common types of pavement surface differs in different urban functional areas, the research may result more practical and instructive if further elements e.g., trip purposes and activity region when using e-kick scooters and e-bikes are considered. Thirdly, the possible relationship among the greater propensity of females than males to injuries from e-kick scooter's crashes and the greater vibrational solicitation acting on the former, coupled with the small diameter of e-kick scooter's wheels, should be experimentally investigated. Lastly, focusing on the relationship between objective and subjective comfort metrics could be beneficial to better understand the distinctions between e-kick scooters and e-bikes, as well as to investigate the possible different level of quality from the user's perspective as applied in other fields (Barabino, 2018).

Declaration of competing interest

The authors declare that they have no known competing financial interests or personal relationships that could have appeared to influence the work reported in this paper.

Acknowledgement

This research was partially funded by POR FESR Lombardia 2014–2020 (project: MoSoRe) and Polis Lombardia with the project "Studi a sostegno delle attività del Centro Regionale di Governo e Monitoraggio della Sicurezza Stradale (CMRL)", code 221313OSS. Furthermore, at the time this article was revised, Roberto Ventura was supported by the Department of Civil, Environmental, Land, and Architecture Engineering and Mathematics (DICATAM) of the University of Brescia through a research grant (CUP code: D73C22000770002).

References

Abdullah, M., Ali, N., Bilal Aslam, A., Ashraf Javid, M., Arif Hussain, S., 2022. Factors affecting the mode choice behavior before and during COVID-19 pandemic in Pakistan. Int. J. Transp. Sci. Technol. 11, 174–186. https://doi.org/10.1016/j.ijtst.2021.06.005.
Almannaa, M.H., Ashqar, H.I., Elhenawy, M., Masoud, M., Rakotonirainy, A., Rakha, H., 2021. A comparative analysis of e-scooter and e-bike usage patterns: findings from the City of Austin, TX. Int. J. Sustain. Transp. 15, 571–579. https://doi.org/10.1080/15568318.2020.1833117.
Alqatawna, A., Rivas Alvarez, A.M., Garcia-Moreno, S.S.C., 2021. Comparison of multivariate regression models and artificial neural networks for prediction highway traffic accidents in spain: a case study. Transp. Res. Procedia 58, 277–284. https://doi.org/10.1016/j.trpro.2021.11.038.
Asperti, M., Vignati, M., Braghin, F., 2021. Modelling of the vertical dynamics of an electric kick scooter. IEEE Trans. Intell. Transp. Syst. 1–9. https://doi.org/10.1109/TITS.2021.3098438.
Azimi, G., Rahimi, A., Lee, M., Jin, X., 2021. Mode choice behavior for access and egress connection to transit services. Int. J. Transp. Sci. Technol. 10, 136–155. https://doi.org/10.1016/j.ijtst.2020.11.004.
Barabino, B., 2018. Automatic recognition of "low-quality" vehicles and bus stops in bus services. Public Transport 10, 257–289. https://doi.org/10.1007/s12469-018-0180-8.
Bíl, M., Andrášik, R., Kubeček, J., 2015. How comfortable are your cycling tracks? A new method for objective bicycle vibration measurement. Transp. Res. Part C Emerg. Technol. 56, 415–425. https://doi.org/10.1016/j.trc.2015.05.007.
Bloom, M., Noorzad, A., Lin, C., Little, M., Lee, E., Margulies, D., Torbati, S., 2020. Standing electric scooter injuries: Impact on a community. Am. J. Surg.
Boglietti, S., Barabino, B., Maternini, G., 2021. Survey on e-powered micro personal mobility vehicles: exploring current issues towards future developments. Sustainability (Switzerland) 13. https://doi.org/10.3390/su13073692.
Boglietti, S., Ghirardi, A., Zanoni, C.T., Ventura, R., Barabino, B., Maternini, G., Vetturi, D., 2022. First experimental comparison between e-kick scooters and e-bike's vibrational dynamics. Transp. Res. Procedia 62, 743–751. https://doi.org/10.1016/j.trpro.2022.02.092.
Cano-Moreno, J.D., Marcos, M.I., Haro, F.B., D'Amato, R., Juanes, J.A., Heras, E.S., 2019. Methodology for the study of the influence of e-scooter vibrations on human health and comfort. PervasiveHealth: Pervasive Comput. Technol. Healthcare, 445–451. https://doi.org/10.1145/3362789.3362906.
Cano-Moreno, J.D., Islán, M.E., Blaya, F., D'Amato, R., Juanes, J.A., Soriano, E., 2021. E-scooter Vibration Impact on Driver Comfort and Health. J. Vib. Eng. Technol. 9, 1023–1037. https://doi.org/10.1007/s42417-021-00280-3.
Carrara, E., Ciavarella, R., Boglietti, S., Carra, M., Maternini, G., Barabino, B., 2021. Identifying and selecting key sustainable parameters for the monitoring of e-powered micro personal mobility vehicles. Evidence from Italy. Sustainability (Switzerland) 13. https://doi.org/10.3390/su13169226.
Chen, H.C., Chen, W.C., Liu, Y.P., Chen, C.Y., Pan, Y.T., 2009. Whole-body vibration exposure experienced by motorcycle riders - An evaluation according to ISO 2631–1 and ISO 2631–5 standards. Int. J. Ind. Ergon. 39, 708–718. https://doi.org/10.1016/j.ergon.2009.05.002.
Chou, C.P., Lee, W.J., Chen, A.C., Wang, R.Z., Tseng, I.C., Lee, C.C., 2015. Simulation of bicycle-riding smoothness by bicycle motion analysis model. J. Transp. Eng. 141, 1–9. https://doi.org/10.1061/(ASCE)TE.1943-5436.0000802.
Cossalter, V., Doria, A., Garbin, S., Lot, R., 2006. Frequency-domain method for evaluating the ride comfort of a motorcycle. Veh. Syst. Dyn. 44, 339–355. https://doi.org/10.1080/00423110500420712.
De Aloe, M., Ventura, R., Bonera, M., Barabino, B., Maternini, G., 2022. Applying cost–benefit analysis to the economic evaluation of a tram-train system: evidence from Brescia (Italy). Res. Transp. Bus. Manage. 47. 100916. https://doi.org/10.1016/j.rtbm.2022.100916.
Enright, B., O'Brien, E.J., 2013. Monte Carlo simulation of extreme traffic loading on short and medium span bridges. Struct. Infrastruct. Eng. 9, 1267–1282. https://doi.org/10.1080/15732479.2012.688753.
Feizi, A., Oh, J.S., Kwigizile, V., Joo, S., 2020. Cycling environment analysis by bicyclists' skill levels using instrumented probe bicycle (IPB). Int. J. Sustain. Transp. 14, 722–732. https://doi.org/10.1080/15568318.2019.1610921.
Flach, P., 2012. Machine Learning: The Art and Science of Algorithms That Make Sense of Data. Cambridge University Press, USA.
Frendo, F., Sgueglia, M., Vitale, E., Hippoliti, R., 2002. Analysis of motorscooter ride comfort. SAE Technical Papers. https://doi.org/10.4271/2002-01-2177.
Gao, J., Sha, A., Huang, Y., Hu, L., Tong, Z., Jiang, W., 2018. Evaluating the cycling comfort on urban roads based on cyclists' perception of vibration. J. Clean Prod. 192, 531–541. https://doi.org/10.1016/j.jclepro.2018.04.275.
Gao, J., Sha, A., Huang, Y., Liu, Z., Hu, L., Jiang, W., Yun, D., Tong, Z., Wang, Z., 2019. Cycling comfort on asphalt pavement: Influence of the pavement-tyre interface on vibration. J. Clean Prod. 223, 323–341. https://doi.org/10.1016/j.jclepro.2019.03.153.
García-Vallejo, D., Schiehlen, W., García-Agúndez, A., 2020. Dynamics, control and stability of motion of electric scooters. Adv. Dyn. Veh. Roads Tracks. https://doi.org/10.1007/978-3-030-38077-9_139.

Garman, C., Como, S.G., Campbell, I.C., Wishart, J., O'Brien, K., McLean, S., 2020. Micro-Mobility Vehicle Dynamics and Rider Kinematics during Electric Scooter Riding. SAE Technical Papers 2020-April. https://doi.org/10.4271/2020-01-0935.

Gharehbaghi, K., 2016. Artificial neural network for transportation infrastructure systems. MATEC Web Conf. 81. https://doi.org/10.1051/matecconf/20168105001.

Istat, 2021. Popolazione residente al 1° gennaio 2021 [WWW Document]. URL http://dati.istat.it/Index.aspx?QueryId=42869.

Repubblica Italiana, 2015. Nuovo codice della Strada - D.Lgs. 285/1992 e s.m. Gazzetta Ufficiale della Repubblica Italiana n. 115 del 3/08/2015 115.

Repubblica Italiana, 2019. DL 30 dicembre 2019, n. 162 - Disposizioni urgenti in materia di proroga di termini legislativi, di organizzazione delle pubbliche amministrazioni, nonche' di innovazione tecnologica. Gazzetta Ufficiale della Repubblica Italiana n.51 del. 29/02/2020.

Repubblica Italiana, 2021. DL 10 settembre 2021, n. 121 - Disposizioni urgenti in materia di investimenti e sicurezza delle infrastrutture, dei trasporti e della circolazione stradale, per la funzionalita' del Ministero delle infrastrutture e della mobilita' sostenibili, del Consiglio superiore dei lavori pubblici e dell'Agenzia nazionale per la sicurezza delle infrastrutture stradali e autostradali. Gazzetta Ufficiale della Repubblica Italiana n.217 del 10/09/2021.

Repubblica Italiana, 2022. Decreto 18 agosto 2022 - Normativa tecnica relativa ai monopattini a propulsione prevalentemente elettrica. Gazzetta Ufficiale della Repubblica Italiana del 30/08/2022.

Jeon, S., Hong, B., 2016. Monte Carlo simulation-based traffic speed forecasting using historical big data. Futur. Gener. Comput. Syst. 65, 182–195. https://doi.org/10.1016/j.future.2015.11.022.

Jiang, Z., Yang, X., Wang, F., Wang, T., 2020. Monte Carlo simulation approach to the duration of yellow lights at signalized intersections considering the stochastic characteristics of drivers. Transp. Res. Record: J. Transp. Res. Board 2674, 37–45. https://doi.org/10.1177/0361198120907890.

Lee, K.J., Yun, C.H., Yun, M.H., 2021. Contextual risk factors in the use of electric kick scooters: an episode sampling inquiry. Saf. Sci. 139. https://doi.org/10.1016/j.ssci.2021.105233.

Lundh, B., 2009. Variation of body weight with age, sex and height: an index for classification of obesity. Acta Med. Scand. 218, 493–498. https://doi.org/10.1111/j.0954-6820.1985.tb08879.x.

Martinelli, V., Ventura, R., Bonera, M., Barabino, B., Maternini, G., 2022. Effects of urban road environment on vehicular speed. Evidence from Brescia (Italy). Transp. Res. Procedia 60, 592–599. https://doi.org/10.1016/j.trpro.2021.12.076.

Maternini, G., 2020. Micromobilità elettrica. EGAF EDIZIONI srl, Forlì.

MathWorks, 2022. Neural Net Fitting - Solve fitting problem using two-layer feed-forward networks [WWW Document]. URL https://it.mathworks.com/help/deeplearning/ref/neuralnetfitting-app.html.

Meijaard, J.P., Papadopoulos, J.M., Ruina, A., Schwab, A.L., 2007. Linearized dynamics equations for the balance and steer of a bicycle: a benchmark and review. Proc. Roy. Soc. A: Math. Phys. Eng. Sci. 463, 1955–1982. https://doi.org/10.1098/rspa.2007.1857.

Mulla, L., Khuba, P., Dhere, A., Palanivelu, S., 2019. Extraction of vibration behavior in conventional and electric drive two-wheeler using order analysis. IOP Conf. Ser. Mater. Sci. Eng. 624. https://doi.org/10.1088/1757-899X/624/1/012009.

Olayode, I.O., Tartibu, L.K., Okwu, M.O., 2021. Prediction and modeling of traffic flow of human-driven vehicles at a signalized road intersection using artificial neural network model: a South African road transportation system scenario. Transp. Eng. 6,. https://doi.org/10.1016/j.treng.2021.100095 100095.

Schmidhuber, J., 2015. Deep learning in neural networks: an overview. Neural Netw. 61, 85–117. https://doi.org/10.1016/j.neunet.2014.09.003.

Shaik, M.E., Islam, M.M., Hossain, Q.S., 2021. A review on neural network techniques for the prediction of road traffic accident severity. Asian Transport Stud. 7,. https://doi.org/10.1016/j.eastsj.2021.100040 100040.

Sharp, R.S., 1971. The stability and control of motorcycles. J. Mech. Eng. Sci.

Stigson, H., Malakuti, I., Klingegård, M., 2021. Electric scooters accidents: analyses of two Swedish accident data sets. Accid. Anal. Prev. 163. https://doi.org/10.1016/j.aap.2021.106466.

Stroeve, S.H., Blom, H.A.P., (Bert), Bakker, G.J., 2009. Systemic accident risk assessment in air traffic by Monte Carlo simulation. Saf. Sci. 47, 238–249. https://doi.org/10.1016/j.ssci.2008.04.003.

Tian, D., Ryan, A.D., Craig, C.M., Sievert, K., Morris, N.L., 2022. Characteristics and risk factors for electric scooter-related crashes and injury crashes among scooter riders: a two-phase survey study. Int. J. Environ. Res. Public Health 19. https://doi.org/10.3390/ijerph191610129.

Tuan Hoang, A., Nižetić, S., Chyuan Ong, H., Tarelko, W., Viet Pham, V., Hieu Le, T., Quang Chau, M., Phuong Nguyen, X., 2021. A review on application of artificial neural network (ANN) for performance and emission characteristics of diesel engine fueled with biodiesel-based fuels. Sustain. Energy Technol. Assess. 47. https://doi.org/10.1016/j.seta.2021.101416.

Tzouras, P.G., Mitropoulos, L., Stavropoulou, E., Antoniou, E., Koliou, K., Karolemeas, C., Karaloulis, A., Mitropoulos, K., Tarousi, M., Vlahogianni, E.I., Kepaptsoglou, K., 2022. Agent-based models for simulating e-scooter sharing services: a review and a qualitative assessment. Int. J. Transp. Sci. Technol. https://doi.org/10.1016/j.ijtst.2022.02.001.

Ventura, R., Barabino, B., Vetturi, D., Maternini, G., 2023. Monitoring vehicles with permits and that are illegally overweight on bridges using Weigh-In-Motion (WIM) devices: a case study from Brescia. Case Stud. Transp Policy 101023. https://doi.org/10.1016/j.cstp.2023.101023.

Vetturi, D., Tiboni, M., Maternini, G., Barabino, B., Ventura, R., 2023. Kinematic performance of micro-mobility vehicles during braking: experimental analysis and comparison between e-kick scooters and bikes. Transp. Res. Procedia 69, 408–415. https://doi.org/10.1016/j.trpro.2023.02.189.

Wach, W., 2014. Monte Carlo method in analysis of road accidents versus interpretation of calculation results. Archiwum Motoryzacji 66 (83–106), 193.

Wang, D., He, B.Y., Gao, J., Chow, J.Y.J., Ozbay, K., Iyer, S., 2021. Impact of COVID-19 behavioral inertia on reopening strategies for New York City transit. Int. J. Transp. Sci. Technol. 10, 197–211. https://doi.org/10.1016/j.ijtst.2021.01.003.

Yang, X., Guan, J., Ding, L., You, Z., Lee, V.C.S., Mohd Hasan, M.R., Cheng, X., 2021. Research and applications of artificial neural network in pavement engineering: a state-of-the-art review. J. Traffic Transp. Eng. (Engl. Ed.) 8, 1000–1021. https://doi.org/10.1016/j.jtte.2021.03.005.

Zagorskas, J., Burinskienė, M., 2020. Challenges caused by Increased Use of E-Powered Personal Mobility Vehicles in European Cities. Sustainability.

Zhang, P., 2010. Industrial control system simulation routines. In: Advanced Industrial Control Technology. Elsevier, pp. 781–810. https://doi.org/10.1016/B978-1-4377-7807-6.10019-1.